Charged Higgs scalar production in the single-top-quark mode (and others) at future ep colliders in the minimal supersymmetric standard model

Stefano Moretti* and Kosuke Odagiri†
Cavendish Laboratory, University of Cambridge, Madingley Road, Cambridge, CB3 0HE, United Kingdom
(Received 6 October 1997; revised manuscript received 8 January 1998; published 6 April 1998)

We study charged Higgs boson production at future electron-proton colliders in the frame-work of the minimal supersymmetric standard model. We focus our attention to the case of single-top-quark production and decay through the channel $t\to bH^\pm$ and of vector-scalar fusion via $W^\pm{}^*\Phi^*\to H^\pm$ (where $\Phi=H$, h, and A). We consider the signature $H^\pm\to\tau\nu_\tau$ and compare it to the irreducible background from standard model interactions. For $M_{H^\pm}\lesssim m_t$, the $H^\pm$ signal is accessible through lepton universality breaking if $M_A \lesssim 100-120$ GeV at both low and large values of tan β. Furthermore, although the bulk of the production cross section comes from single-top-quark events, a sizable contribution due to vector-scalar-scalar interactions should be observable at large tan β, this possibly offering some insight into the structure of the scalar sector of the theory. The possibility of the CERN collider running in the LEP⊕LHC mode is considered in detail. [S0556-2821(98)06209-2]

PACS number(s): 13.85.Hd, 12.60.Jv, 14.65.Ha, 14.80.Cp

I. INTRODUCTION AND MOTIVATION

A charged Higgs boson is an essential component of the two Higgs doublet models, which includes supersymmetry (SUSY) and technicolor theories [1]. Such a particle does not belong to the spectrum of the standard model (SM) and therefore its detection would indicate new physics.

Within the minimal supersymmetric standard model (MSSM), a lower limit on the value of its mass has been set at ≈ 100 GeV by the data from the CERN e^+e^- collider LEP 2 yielding $M_A \gtrsim 60$ GeV (for tan $\beta \gtrsim 1$) [2]. The unitarity of the underlying theory sets the upper limit in the TeV region [3]. Therefore, the MSSM mass range allowed for the existence of charged Higgs bosons is vast. However, if one assumes that the mass scale of the MSSM partners of ordinary matter is above the $H^\pm$ one, then only two modes dominate the decay phenomenology of the charged Higgs boson, their reciprocal relevance depending on the value of the top quark mass [4]. If $M_{H^\pm}\lesssim m_t$, the branching ratio (B) $B(H^\pm\to\tau\nu_\tau)$ is the largest (around 98%, for tan $\beta>2$) and depends only slightly on the β angle. When $M_{H^\pm}\gtrsim m_t$, the $H^\pm\to bt$ decay mode is the only accessible channel (with a B of practically 100% at all tan β's).

As for the production mechanisms of charged Higgs bosons of the MSSM at colliders, it is likely that one will have to wait for the advent of the future generation of high energy accelerators, in order to detect such particles. In fact, at LEP2, the huge irreducible background in $e^+e^-\to W^+W^-$ events renders the signal $e^+e^-\to H^+H^-$ [5] very hard to extract. In addition, the discovery potential of such a machine is now confined to a tiny window of a few GeV and only if $\sqrt{s_{ee}}\approx 205$ GeV [6].

At the CERN Large Hadron Collider LHC [7,8], the charged Higgs scalar of the MSSM should be easily accessible (via $H^\pm\to\tau\nu_\tau$: the lepton universality breaking signal) if $m_t\gtrsim M_{H^\pm}$, since $H^\pm$'s will be copiously produced in top quark decays (here, $m_t=175$ GeV). If $M_{H^\pm}\gtrsim m_t$, the chances of detection at the LHC are very much reduced, as in this case only the subprocesses $bg\to tH^\pm$ [9] and $bq\to bq'H^\pm$ [10] can be of some help, provided $M_{H^\pm}\lesssim 300-400$ GeV [1] (at large values of tan β in the second case). Furthermore, the signature to be extracted would be $H^\pm\to bt\to b\bar{b}W^\pm\to b\bar{b}jj$ (where j represents a jet from the $W^\pm$ decay), which relies on very high b-tagging performances and jet resolution to reduce the QCD noise [11].

At the Next Linear Collider (NLC) [12], $H^\pm$ detection looks promising in the low $H^\pm$ mass range [13]. Once again the crucial point is the heavy mass range: in this case the maximum center-of-mass (c.m.) energy sets the upper limit on the detectable $H^\pm$ mass. For a $\sqrt{s_{ee}}=500$ GeV NLC [12], one has $M_{H^\pm}^{\max}\approx 220$ GeV, as the main production channel is $e^+e^-\to H^+H^-$ [5]. Furthermore, the $e^\pm\gamma$ and $\gamma\gamma$ running modes [14] at the NLC do not improve the prospects of MSSM charged Higgs boson detection [15]: they only allow one to cover adequately the intermediate Higgs boson mass range.

Since the detection of heavy charged Higgs scalars of the MSSM is far from certain even after the end of the LHC and NLC era, it is worthwhile to assess the discovery potential of these particles at other planned and proposed machines (see [16] for a review). The hope is that these could extend the present coverage in mass of MSSM charged Higgs scalars, possibly involving new interactions other than the $t\to bH^\pm$ decay (LHC) and the QED-like vertex $\gamma\to H^+H^-$ (NLC).

We turn our attention to the case of future electron (positron)-proton colliders, running with a c.m. energy in the TeV range.[1] The physics of ep colliders, in conjunction with

*Email address: moretti@hep.phy.cam.ac.uk
†Email address: odagiri@hep.phy.cam.ac.uk

[1]The charged Higgs boson discovery potential of the only ep collider operative at present, i.e., the DESY ep collider HERA, has been shown to be very poor [17]: the production rates are significant only for very light scalar masses (now ruled out by experiment) [18].

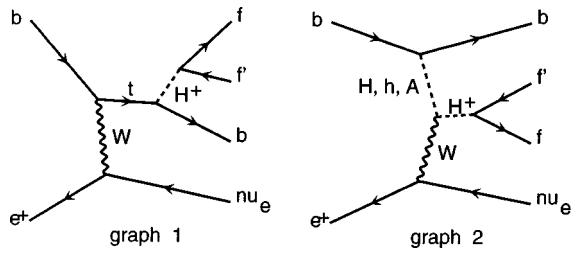

FIG. 1. Lowest order Feynman diagrams describing processes (4). Graph 1 refers to single-top-quark production and decay whereas graph 2 corresponds to the vector-scalar fusion mechanism.

the discussed possibility of their running in the γp mode [19], has been recently under renewed and active discussion [20], also motivated by the current large Q^2 anomaly [21]. A possible design was proposed and several experimental simulations performed already in 1990 [22], for a LEP⊕LHC [23] machine obtainable crossing an electron (positron) beam from LEP with a proton beam from the LHC [24,25].

To our knowledge, no detailed study of MSSM charged Higgs boson production at future ep colliders exists in the literature, apart from a preliminary analysis carried out in Ref. [26]. However, we do expect that charged Higgs bosons of the MSSM can be abundantly produced in electron (positron)-proton collisions at the TeV scale. In particular, it is the purpose of this paper to study the reaction (e.g., for the case of a positron beam)

$$e^+ b \to \overline{\nu}_e b H^+, \tag{1}$$

proceeding through the two subprocesses

$$e^+ b \to \overline{\nu}_e t \to \overline{\nu}_e b H^+ \tag{2}$$

(i.e., single-top-quark production and decay) and (with $\Phi = H$, h and A)

$$e^+ b \to \overline{\nu}_e W^{\pm} * \Phi * \to \overline{\nu}_e b H^+ \tag{3}$$

(i.e., vector-scalar fusion). If one considers two-body fermion decays of the charged Higgs boson then the graphs contributing to

$$e^+ b \to \overline{\nu}_e b H^+ \to \overline{\nu}_e b f \overline{f'} \tag{4}$$

(where ff' represents, e.g., $\tau^+ \nu_\tau$ or bt) are those depicted in Fig. 1.

We are motivated to study this process following the results presented in Ref. [10], where the hadronic counterpart of process (4) was considered (i.e., $e^+ \to q$ and $\overline{\nu}_e \to q'$, with $q^{(\prime)}$ light quark). There, it was shown that bq fusion could effectively help in increasing the chances of $H^{\pm}$ detection at the LHC, also above the $H^{\pm} \to bt$ decay threshold. This is due to three reasons: (i) a large component of b quarks inside the proton; (ii) the strength of the Yukawa couplings of the neutral Higgs bosons of the MSSM to the b quarks increasing with the value of $\tan\beta$ (graph 2); (iii) very high vertex tagging performances of the LHC detectors. One should expect this channel to be similarly effective also at a future ep collider, as the large content of heavy quarks inside the scattered hadron is guaranteed by the TeV energy and the capabilities of the LHC vertex detector should be maintained while running the CERN machine in the ep mode. Along with the signal (1) we will also study several SM-like ''irreducible'' backgrounds, on the same footing as in Ref. [10].

The plan of the paper is as follows. In the next section we discuss some details of the calculation. Section III presents our results whereas in the last section we outline some brief conclusions.

II. PARAMETERS

As for the details of the computation techniques of the relevant Feynman amplitudes, for the choice of structure functions as well as for the numerical values of the SM parameters used in this paper, we refer the reader to Ref. [28] [see also Ref. [10] for an analytical expression of the matrix element of the hard scattering process (1)]. Contrary to Ref. [28], for the present analysis we adopt the unique ''running value'' $\mu = \sqrt{\hat{s}}$ for both α_s and the factorization/renormalization scale μ of the parton distribution functions (PDFs). Another difference with respect to Ref. [28] is the expression used for the top quark width, which has been modified in order to allow for SUSY decays of the top quark.

Concerning the MSSM parameters, we assume a universal soft supersymmetry-breaking mass [29] and negligible mixing in the stop and sbottom mass matrices. Under these conditions, the one-loop corrections reduce to simple formulas, which we have already recalled in Ref. [10]. For the MSSM charged Higgs boson mass we have maintained the tree-level relation $M^2_{H^{\pm}} = M^2_{W^{\pm}} + M^2_A$, since one-loop corrections are small. As it is impractical to cover all possible regions of the MSSM parameter space (M_A, $\tan\beta$), we have decided to concentrate here on the two representative values $\tan\beta = 1.5$ and 30. and on masses of the pseudoscalar Higgs boson A in the range $60\ \text{GeV} \lesssim M_A \lesssim 220\ \text{GeV}$.

As was done in Ref. [28], we consider (as an illustration, see the discussion there) the case of positron beams from LEP (i.e., of $e^+ b$ fusion). The total c.m. energy $\sqrt{s_{ep}}$ of the colliding particles will span in the range between 300 GeV (i.e., around the HERA value) and 2 TeV. However, we will focus our attention mainly to the case of a possible LEP2⊕LHC accelerator, with a 100 GeV electron (positron) and a 7 TeV proton, so that the total energy in the frame of the colliding particles would be $\sqrt{s_{ep}} \approx 1.7$ TeV. Depending on the relative values of the electron (positron) and proton energy, the instantaneous luminosity should vary in the range $(5 \times 10^{31} - 4 \times 10^{32})\ \text{cm}^{-2}\,\text{s}^{-1}$ [30]. We convert these values into $1\ \text{fb}^{-1}$ of integrated luminosity per annum, which we will adopt as the default in forthcoming discussions.

Before proceeding with the discussion of the results, we present in Table I the cross sections of the signal process (1) evaluated at the LEP2⊕LHC energy for several up-to-date sets of PDFs. This is done in order to estimate a ''lower limit'' (see Ref. [28]) on the theoretical error due to the b in the initial state. We found the PDF dependence of process (1) to be less than 25%, a quite small error already at the present time.

III. RESULTS

We show the production and decay rates for process (1) in Figs. 2 and 3. Generally the cross section at $\tan\beta = 30$ [Fig.

TABLE I. Total cross sections for process (1) for various sets of structure functions. Numerical errors arise from the Monte Carlo integration. As representative values of the MSSM parameters we have used $M_A=60$ GeV and $\tan\beta=1.5$.

$\sigma(e^+b\to\overline{\nu}_e bH^+)$	
PDFs	σ_t (fb)
MRS(A)	752.3 ± 2.0
MRS(A')	739.5 ± 1.9
MRS(G)	716.9 ± 1.9
MRS($R1$)	701.0 ± 1.9
MRS($R2$)	757.8 ± 2.1
MRS($R3$)	716.4 ± 1.9
MRS($R4$)	766.9 ± 2.0
MRRS(1)	804.4 ± 2.2
MRRS(2)	805.9 ± 2.2
MRRS(3)	803.2 ± 2.2
CTEQ(2M)	782.5 ± 2.1
CTEQ(3M)	832.9 ± 2.3
CTEQ(4M)	815.0 ± 2.3
CTEQ(4HQ)	891.2 ± 2.5
no acceptance cuts	
LEP2⊕LHC	

2(b)] is greater than that at 1.5 [Fig. 2(a)]. This is because the contribution to the total rate of subprocess (3) is negligible at $\tan\beta=1.5$ and also because the top B into $bH^\pm$ pairs is higher at larger $\tan\beta$'s. These features can be easily traced back in terms of the strength of the scalar-fermion vertices involved [1]. Figure 2(c)–2(d) illustrate the relative relevance of the subprocess (3) in the total production rates.

Figure 3(a) emphasizes the point that, at LEP⊕LHC energies and for a yearly luminosity of 1 fb^{-1}, a charged Higgs particle of less than the top quark mass (i.e., $M_A \lesssim 140$ GeV) can be abundantly produced. For $M_A \gtrsim 140$ GeV, the rate begins to be very small with a strong decrease of the cross sections for an increasing Higgs boson mass.

The dependence of the production rates on the c.m. energy $\sqrt{s_{ep}}$ is governed by the kinematic suppression on the single-top-quark production and at low energies, say $\sqrt{s_{ep}} \lesssim 500$ GeV, the cross section falls to negligible scales for all combinations in the plane (M_A,$\tan\beta$). In general, although the rate of process (1) is small at existing collider energies, it increases markedly near the TeV scale. At the LEP2⊕LHC energy it is easily observable already after one year of running as long as single-top production dominates. When this is no longer the case (i.e., when $M_{H^\pm} \gtrsim m_t$), production rates fall below the 1 fb detection level. Thus, the discovery potential of future ep colliders is confined to the intermediate $M_{H^\pm}$ range only, where the coverage furnished by the LHC and the NLC will probably be more than adequate.

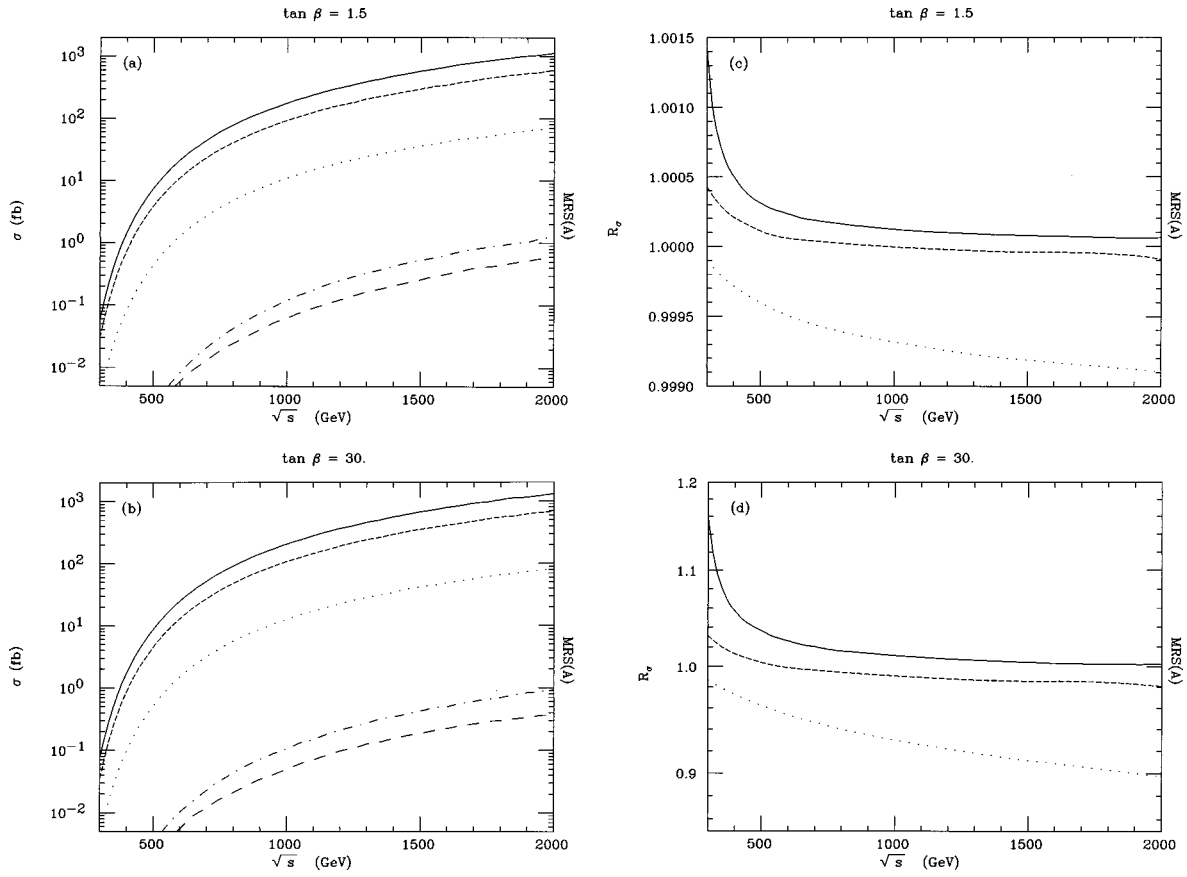

FIG. 2. The total cross section σ for process (1) [(a),(b)] and the ratio R_σ between this and that of process (2) [(c),(d)] as a function of the energy $\sqrt{s_{ep}}$ for two values of $\tan\beta$ and for five pseudoscalar Higgs boson masses: $M_A=60$ GeV (continuous lines), $M_A=100$ GeV (short-dashed lines), $M_A=140$ GeV (dotted lines), $M_A=180$ GeV (dot-dashed lines) and $M_A=220$ GeV (long-dashed lines).

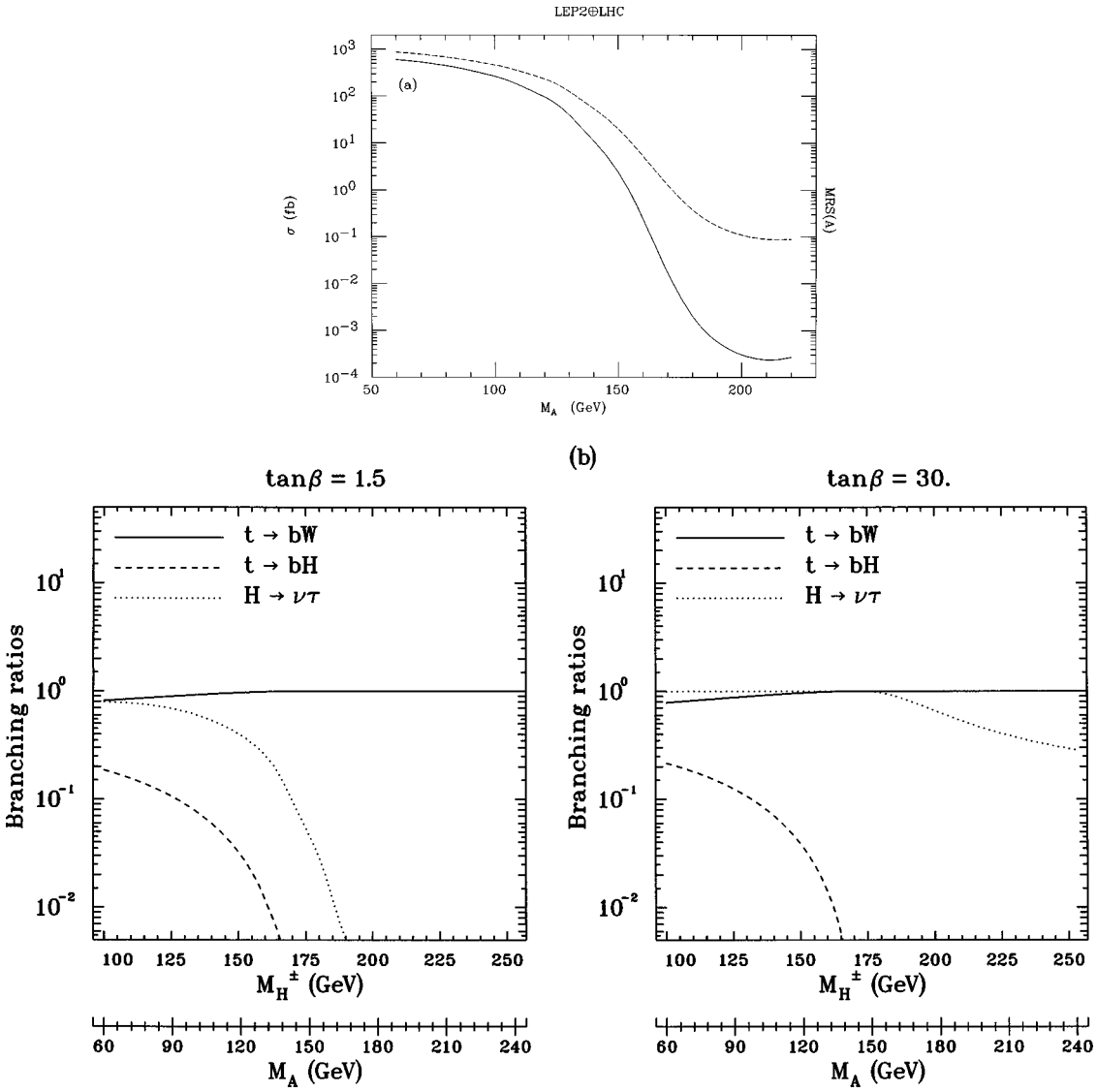

FIG. 3. (a) The total cross section for process (5) as a function of the pseudoscalar Higgs boson mass for tan β=1.5 (continuous line) and tan β=30 (dashed line). (b) The B of the top quark and charged Higgs boson as a function of the charged (pseudoscalar) Higgs boson mass in the range 100(60)GeV$\lesssim M_{H^\pm}(M_A)\lesssim$252(240)GeV for two values of tan β.

However, the production mechanism here is different, as it also proceeds (other than via top quark decays) through diagrams involving the neutral Higgs bosons whose effects are perceptible over a sizable portion of the MSSM parameter space, provided tan β is large enough [compare Fig. 2(c) to Fig. 2(d)]. This is particularly true at small values of $\sqrt{s_{ep}}$ (where the $t\to bH^\pm$ channel is suppressed by the phase space: i.e., $\sqrt{\hat{s}}\sim m_t$) and M_A. At those energies, however, the total cross section of process (1) is too low. In contrast, this is no longer the case at LEP2⊕LHC energies, where the effects of graph 2 are still significant (for large tan β's) and act on a comfortably large total cross section. On its own, subprocess (3) yields (at $\sqrt{s_{ep}}\approx$1.7 TeV) a rate of approximately 2 fb (for M_A=140 GeV and tan β=30). However, a somewhat stronger effect appears through the (negative) interference between the two graphs in Fig. 1, reducing the single-top-quark rates by -10% or so. This is presumably the effect to search for, as it will probably not be possible to separate the two components (2)–(3) of the cross section efficiently: the charged Higgs bosons produced decay leptonically (with the neutrinos escaping the detectors) and the $t\to bH^\pm$ resonance cannot be reconstructed and exploited to remove single-top-quark events. For 1 fb^{-1} of yearly luminosity, the above rates mean that some 5 events out of the 59 expected from single-top-quark production should be missing.[2] Such an effect could well be used to test possible anomalous couplings in the Higgs sector of the MSSM and/or in constraining possible gauge violations affecting the $W^\pm\Phi H^\pm$ vertex.

In the remainder of the paper, since the only $H^\pm$ mass range that can be explored at future TeV ep colliders is

[2]Note that, if the electron (positron) beam will have a 50 GeV energy, this yielding $\sqrt{s_{ep}}\approx$1.2 TeV, so to increase the luminosity (see Ref. [23]) by a factor of ten, one would then rely on a statistically more significative sample, as at that energy the depletion due to interference effects is around 8%. However, we do not consider here such a possibility.

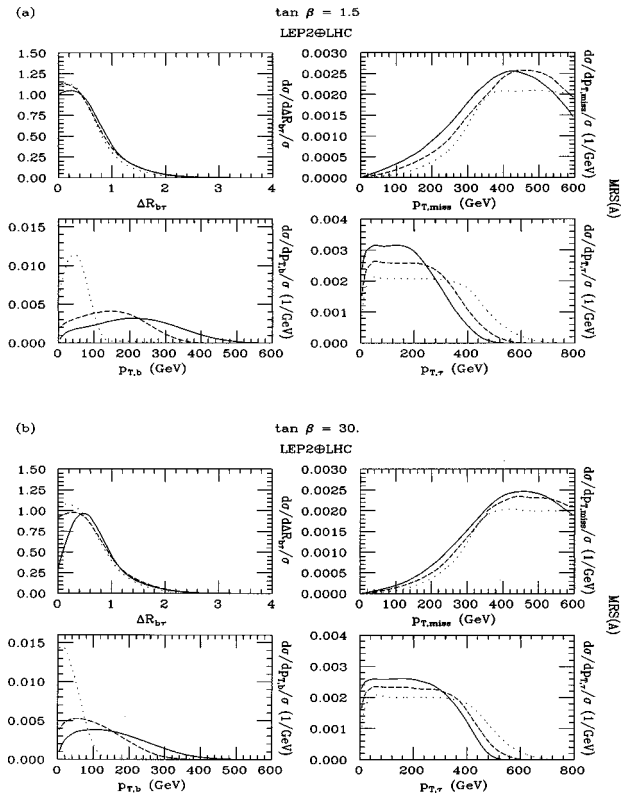

FIG. 4. Differential distributions for process (5) in the following variables (clockwise): (1) $\Delta R_{b\tau}$, the azimuthal-pseudorapidity separation of the $b\tau$ pair; (2) $p_{T,miss}$, the missing transverse momentum; (3) $p_{T,\tau}$, the transverse momentum of the τ lepton; (4) $p_{T,b}$, the transverse momentum of the b quark; for tan β=1.5 (a) and 30 (b) and for three different values of the pseudoscalar Higgs boson mass: M_A=60 GeV (continuous lines), M_A=100 GeV (dashed lines), and M_A=140 GeV (dotted lines). The normalization is to unity.

below m_t, we will consider $\tau\nu_\tau$ decays of the charged Higgs boson only: that is, the two-to-four body reaction

$$e^+ b \to \overline{\nu}_e b H^+ \to \overline{\nu}_e b \nu_\tau \tau^+ . \tag{5}$$

The signature that one should expect from this process would then be a τ jet (which we assume easily distinguishable from those originated by quarks and gluons), a b jet (which we assume to be vertex tagged with efficiency close to unity) and appreciable missing momentum, and the signal should be revealed as a clear lepton universality breaking excess with respect to the rates due to SM processes.

Figures 4(a)–4(b) plots the differential distributions in various kinematic quantities which can be reconstructed from the detectable particles in the final state of process (5). The distribution in transverse momenta p_T shows that neither cuts in p_T nor cuts in $p_T^{\rm miss}$ will affect the total cross section dramatically, whereas that of ΔR, the azimuthal-pseudorapidity separation defined by $\Delta R = \sqrt{(\Delta\phi)^2+(\Delta\eta)^2}$ (where ϕ is the azimuthal angle and η the pseudorapidity) indicates that the requirement of an isolated lepton may strongly affect the event rate. The majority of events are found within $\Delta R \lesssim 1.5$, which is about 90 degrees in the azimuthal angle. This is because the bottom quark jet and the tau come from the energetic top quark.

TABLE II. Total cross section for process (5) for a selection of Higgs boson masses. Numerical errors arise from the Monte Carlo integration. The following acceptance cuts were implemented: (i) $p_T^{\tau^+}$, $p_T^b > 20$ GeV, $p_T^{miss} > 10$ GeV, and $\Delta R_{\tau^+,b} > 0.7$.

	$\sigma_{\rm tot}$ signal (fb)	
M_A (GeV)	tan β=1.5	tan β=30
60	194.66±0.87	327.1±1.7
80	140.66±0.62	243.9±1.3
100	76.95±0.40	149.12±0.80
120	24.28±0.14	62.40±0.36
140	2.122±0.010	8.656±0.065
	after acceptance cuts	
LEP2⊕LHC		MRS(A)

Thus, at lower energies the azimuthal-pseudorapidity spread in the top quark decay products will be larger and hence the requirement of an isolated lepton not so severe. The distribution of the missing transverse momentum is small at low missing p_T and indicates that the charged current cut in missing transverse momentum will not affect the event rate significantly.

Table II shows the total cross section after the acceptance cuts. The following constraints were implemented (see [27] for discussions): $p_T^{\tau^+}$, $p_T^b > 20$ GeV, $p_T^{\rm miss} > 10$ GeV, and $\Delta R_{\tau^+,b} > 0.7$. We have not implemented any cuts on the pseudorapidity, as the events are all concentrated in the detectable $|\eta|$ region: see the spectra in the two lower frames of Figs. 5(a) and 5(b).

In Figs. 5(a) and 5(b) we also plot the distributions in the invariant mass of the only visible pair of particle momenta, the b and τ ones, i.e., $M_{b\tau}$. This is done in order to possibly aid further the signal selection, as this cannot rely on the kinematic reconstruction of the charged Higgs boson mass, because of the τ neutrino. In particular we would like to point out that there is a kinematic interplay between, on the one hand, the top quark, tau and bottom quark masses and, on the other hand, that of the boson produced in the top quark decay, inducing a cutoff on the maximum value of $M_{b\tau}$. This should clearly be different for the ordinary SM-like backgrounds, particularly that due to single-top production followed by $t \to bW^\pm$ (the dominant one, see Ref. [28]). In general, assuming that both the top quark and the decay boson are on-shell, the cutoff is given by $M_{b\tau}^{\rm max} = \sqrt{m_t^2+m_b^2+m_\tau^2-M_V^2}$, with $M_V = M_{H^\pm}$ or $M_{W^\pm}$. For example, at low M_A, the cutoff in the roughly triangular distributions in $M_{b\tau}$ is close to the top quark mass as expected, whereas at high M_A, as the charged Higgs boson mass tends to the top quark mass, the cutoff is smaller since the momenta carried by the bottom quark become less energetic. For comparison, in Fig. 6 we present the same $M_{b\tau}$ distribution for the background processes

$$e^+ b \to \overline{\nu}_e b \tau^+ \nu_\tau , \tag{6}$$

and

$$e^+ \overline{b} \to \overline{\nu}_e \overline{b} \tau^+ \nu_\tau , \tag{7}$$

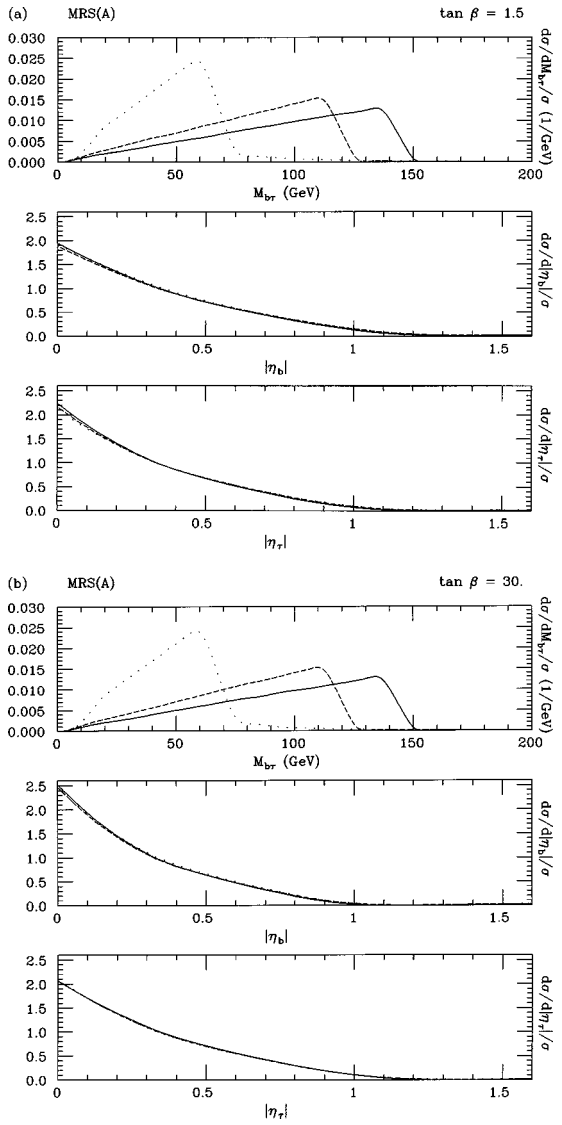

FIG. 5. Differential distributions for process (5) in the following variables (from top to bottom): (1) $M_{b\tau}$, the invariant mass of the $b\tau$ pair; (2) $|\eta_b|$, the absolute value of the pseudorapidity of the b quark; (3) $|\eta_\tau|$, the absolute value of the pseudorapidity of the τ lepton; for $\tan\beta=1.5$ (a) and 30 (b) and for three different values of the pseudoscalar Higgs boson mass: $M_A=60$ GeV (continuous lines), $M_A=100$ GeV (dashed lines), and $M_A=140$ GeV (dotted lines). The normalization is to unity.

both proceeding via a $W^{+(*)}\to\tau^+\nu_\tau$ splitting (see Figs. 1c and d of Ref. [28], respectively). To facilitate the comparison between the two figures, the normalization has been set to unity. We see that the spectrum of the MSSM signal is significantly harder (softer) than the SM-like one from process (6) for smaller (larger) values of M_A, at all $\tan\beta$. There is a sort of degeneracy between the two processes (5) and (6) for $M_A=100$ GeV. This is due to the additional diagrams entering in the latter reaction, which do not suffer from the kinematic cutoff. Also note that for the background there is no dependence of the shape on the actual values of the MSSM parameters. As for events of the type (7), the distribution is rather flat, with no evident kinematic peak. Thus, apart for $M_A\approx100$ GeV, the $M_{b\tau}$ spectrum should indeed help in disentangling the $H^\pm$ signals from the irreducible background.

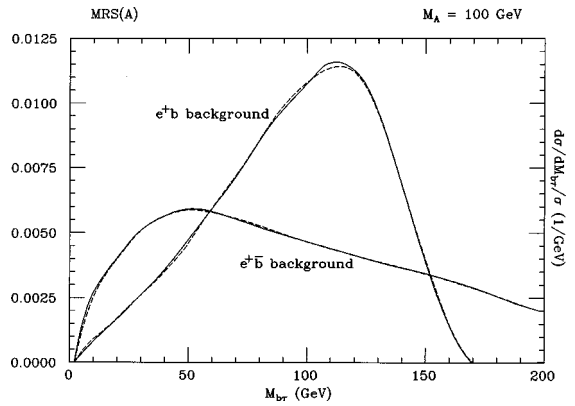

FIG. 6. Differential distributions in the invariant mass of the $b\tau$ pair, $M_{b\tau}$, for processes (6) (e^+b background) and (7) ($e^+\bar{b}$ background) for $M_A=100$ GeV, $\tan\beta=1.5$ (solid lines), and $\tan\beta=30$ (dashed lines). The normalization is to unity.

The total cross sections of process (6) are presented in Table III, for the same choice of the (M_A,$\tan\beta$) parameters as in the previous one. We do not reproduce here the rates for process (7) as these are two orders of magnitude smaller and with no dependence on M_A and/or $\tan\beta$, confirming that the background that does not involve the on-shell top quark production will not affect the detection of $H^\pm$ signals at all, even in case of poor performances in measuring the jet charge of the b jet. The dependence of the background (6) on the MSSM parameters can be traced back to the simple fact that the greater the B for the top decay into $H^\pm$ the smaller the B for the background process $t\to bW^+$. The dependence entering in the total cross section of process (6) through the neutral Higgs mediated diagrams (see Fig. 1c of Ref. [28]) is indeed negligible.

It can be seen that for $\tan\beta=1.5$ the lepton universality breaking signal is significant over the background for M_A up to about 100 GeV, whereas at $\tan\beta=30$ the signal is significant up to 120 GeV. Therefore, a combination of event rate counting and $M_{b\tau}$ distribution studies should allow for the detection of charged Higgs bosons of the MSSM over a large portion of the ($M_A\tan\beta$) plane.

IV. CONCLUSIONS

We conclude that future ep colliders operating in the TeV range have the potential for detecting the charged Higgs sca-

TABLE III. Total cross section for process (6) for a selection of Higgs boson masses. Numerical errors arise from the Monte Carlo integration. The following acceptance cuts were implemented: (i) $p_T^{\tau^+}$, $p_T^b>20$ GeV, $p_T^{miss}>10$ GeV, and $\Delta R_{\tau^+,b}>0.7$.

	$\sigma_{\rm tot}e^+b$ background (fb)	
M_A (GeV)	$\tan\beta=1.5$	$\tan\beta=30$
60	349.1 ± 3.6	341.3 ± 3.7
80	374.6 ± 4.1	358.1 ± 4.3
100	390.9 ± 4.3	384.5 ± 4.6
120	416.6 ± 4.7	413.4 ± 5.0
140	446.5 ± 6.9	439.9 ± 6.3
	after acceptance cuts	
LEP2⊕LHC		MRS(A)

lar of the MSSM for $M_{H^\pm} \lesssim m_t$, by exploiting the signature involving $\tau\nu_\tau$ pairs. Although for such values of $M_{H^\pm}$ the event rate is primarily due to top quark decays (such as at the LHC), the latter being produced in the charged current process $e^+b \to \bar{\nu}_e t \to \bar{\nu}_e b H^+$, the additional feature at ep colliders is a sizable contribution from the vector-scalar fusion $e^+b \to \bar{\nu}_e b W^{\pm *} \Phi^* \to \bar{\nu}_e b H^+$ involving all the neutral Higgs bosons of the MSSM (i.e., $\Phi = H,h,A$), provided $\tan\beta$ is large. For values of $M_{H^\pm}$ in the heavy range, the single-top-quark production rates fall at negligible levels and the kinematic suppression on the vector-fusion mechanism is such that the production cross section is below detection level, even for optimistic luminosities. Therefore, as for heavy charged Higgs bosons of the MSSM, no further $H^\pm$ detection potential other than that already provided by the LHC and/or NLC should be expected at future ep accelerators.

In summary, we believe that charged Higgs boson phenomenology in the context of the MSSM can be a relevant experimental issue at future ep colliders, and we look forward to more detailed simulations, including detector and hadronization effects [31].

ACKNOWLEDGMENTS

We thank Lorenzo Diaz-Cruz for useful discussions. S.M. is grateful to the UK PPARC and K.O. to Trinity College and the Committee of Vice-Chancellors and Principals of the Universities of the United Kingdom for financial support. S.M. also thanks the Theoretical Physics Department in Lund (Sweden), where part of this work was carried out under a grant of the Italian Institute of Culture ''C.M. Lerici'' (Ref. No.: Prot. I/B1 690).

[1] J. F. Gunion, H. E. Haber, G. L. Kane, and S. Dawson, *The Higgs Hunter Guide* (Addison-Wesley, Reading, MA, 1990).
[2] See, e.g., ALEPH Collaboration, R. Barate *et al.*, Phys. Lett. B **412**, 173 (1997).
[3] P. Langacker and H. A. Weldon, Phys. Rev. Lett. **52**, 1377 (1984); H. A. Weldon, Phys. Rev. D **30**, 1547 (1984); Phys. Lett. **146B**, 59 (1984).
[4] S. Moretti and W. J. Stirling, Phys. Lett. B **347**, 291 (1995); **366**, 451E (1996).
[5] A. Djouadi, J. Kalinowski, and P. M. Zerwas, Z. Phys. C **57**, 569 (1993); S. Komamiya, Phys. Rev. D **38**, 2158 (1988).
[6] S. Moretti and K. Odagiri, J. Phys. G **23**, 537 (1997).
[7] ATLAS Technical Proposal, CERN/LHC/94-43 LHCC/P2, December 1994.
[8] CMS Technical Proposal, CERN/LHC/94-43 LHCC/P1, December 1994.
[9] J. F. Gunion, H. E. Haber, F. E. Paige, W.-K. Tung, and S. S. D. Willenbrock, Nucl. Phys. **B294**, 621 (1987).
[10] S. Moretti and K. Odagiri, Phys. Rev. D **55**, 5627 (1997).
[11] J. F. Gunion, H. E. Haber, S. Komamiya, H. Yamamoto, and A. Barbaro-Galtieri, in *Proceedings of the 1987 Berkeley Workshop on Experiments, Detectors and Experimental Areas for the Supercollider*, edited by R. Donaldson and M. Gilchriese (World Scientific, Singapore, 1988).
[12] *e^+e^- Collisions at 500 GeV. The Physics Potential*, Proceedings of the Workshop, Munich, Annecy, Hamburg, edited by P. M. Zerwas (DESY Report No. 92-123 A/B/C, Hamburg, 1992–1993); *Physics with e^+e^- Colliders*, Proceedings of the Workshop, Annecy, Gran Sasso, Hamburg, edited by P. M. Zerwas (DESY Report No. 97-100, Hamburg, 1997).
[13] A. Sopczak, in Ref. [12], part C.
[14] W. Kozanecki (convener), in Ref. [12], part B; E. Boos, P. Bussey, G. Jikia, D. J. Miller, and J. K. Storrow (conveners), in Ref. [12], part C.
[15] J. F. Gunion and H. E. Haber, report UCD-90-25, 1990 (unpublished); in *Research Directions for the Decade*, Proceedings of the Summer Study on High Energy Physics, Snowmass, Colorado, 1990, edited by E. L. Berger (World Scientific, Singapore, 1991); S. Moretti, Phys. Rev. D **50**, 2016 (1994); D. Bowser-Chao, K. Cheung, and S. Thomas, Phys. Lett. B **315**, 399 (1993).
[16] J. Ellis, Plenary Talk presented at the Europhysics Conference on High Energy Physics, Jerusalem, August 1997, Report No. CERN-TH/97-367, December 1997.
[17] See, e.g., *Future Physics at HERA*, Proceedings of the Workshop, edited by G. Ingelman, A. De Roeck, and R. Klanner (DESY, Hamburg, 1995–1996).
[18] I. S. Choi, B. H. Cho, B. R. Kim, and R. Rodenberg, Phys. Lett. B **200**, 200 (1988); B. Grzadkowski and W.-S. Hou, *ibid.* **210**, 233 (1988); T. Han and C. Liu, Z. Phys. C **28**, 295 (1985).
[19] G. Abu Leil and S. Moretti, Phys. Rev. D **53**, 178 (1996).
[20] *Linac-Ring Type ep and Gamma-p Colliders*, Proceedings of the International Workshop, Ankara, Turkey, 1997 (unpublished).
[21] See, e.g., E. Elsen, Plenary Talk presented at the Europhysics Conference on High Energy Physics, Jerusalem, 1997 (unpublished).
[22] *Proceedings of the ECFA Large Hadron Collider Workshop*, Aachen, Germany, edited by G. Jarlskog and D. Rein (CERN Report No. 90-10, ECFA Report No. 90-133, Geneva, Switzerland, 1990).
[23] Rückl, [22], Vol. I.
[24] Verdier [22], Vol. III.
[25] E. Keil, LHC Project Report 93 (1997).
[26] J. L. Diaz-Cruz and O. A. Sampayo, Report No. UAB-FT-286/92, 1992 (unpublished).
[27] A. Ali, F. Barreiro, J. F. de Trocóniz, G. A. Schuler, and J. J. van der Bij, in Ref. [22], Vol. II.
[28] S. Moretti and K. Odagiri, Report No. Cavendish-HEP-97/04, 1997.
[29] Y. Okada, M. Yamaguchi, and T. Yanagida, Prog. Theor. Phys. Suppl. **85**, 1 (1991); J. Ellis, G. Ridolfi, and F. Zwirner, Phys. Lett. B **257**, 83 (1991); **262**, 477 (1991); H. E. Haber and R. Hempfling, Phys. Rev. Lett. **66**, 1815 (1991); R. Barbieri and M. Frigeni, Phys. Lett. B **258**, 395 (1991); A. Brignole, J. Ellis, G. Ridolfi, and F. Zwirner, *ibid.* **271**, 123 (1991); A. Brignole, *ibid.* **277**, 313 (1992); H. E. Haber and M. A. Diaz, Phys. Rev. D **45**, 4246 (1992); V. Barger, K. Cheung, R. J. N. Phillips, and A. L. Stange, *ibid.* **46**, 4914 (1992).
[30] Feltesse, [22], Vol. I.
[31] G. Ingelman, J. Rathsman, and G. A. Schuler, Comput. Phys. Commun. **101**, 135 (1997) (and references therein).